Skyrmion dynamics and disintegration in a spin-1 Bose-Einstein condensate

Xiao-Qiang Xu[1,2] and Jung Hoon Han[1,3,*]

[1]*Department of Physics and BK21 Physics Research Division, Sungkyunkwan University, Suwon 440-746, Korea*

[2]*Department of Physics, Hangzhou Normal University, Hangzhou 310036, China*

[3]*Asia Pacific Center for Theoretical Physics, POSTECH, Pohang, Gyeongbuk 790-784, Korea*

(Received 5 July 2012; published 17 December 2012)

Dynamics of skyrmionic spin texture in the spin-1 Bose-Einstein condensate is examined by analytical and numerical means. We show the skyrmion (coreless vortex) to be inherently unstable in the sense that the state initially prepared purely within the antiferromagnetic (ferromagnetic) order parameter manifold inevitably evolves into a mixture of both. The vorticity-dependent drift in the presence of the trapping potential also contributes to the disintegration of the initial spin texture manifold. We argue that the notion of a skyrmion as a topologically protected entity becomes ill defined during the dynamical evolution process.

DOI: 10.1103/PhysRevA.86.063619 PACS number(s): 03.75.Mn, 03.75.Kk, 05.30.Jp, 67.85.Jk

I. INTRODUCTION

Optical traps enable the possibility to host more than one hyperfine spin state of cold atoms simultaneously, therefore opening up the popular study of spinor Bose-Einstein condensate (BEC) since the first experimental realization [1]. The pioneering theories of the spin-1 BEC worked out by Ho [2], and independently by Ohmi and Machida [3], made possible the understanding of the ground-state structures as either antiferromagnetic (AFM) or ferromagnetic (FM) and elementary excitations. Besides the equilibrium properties, the dynamical behaviors also received great experimental attention [4] later on, breeding new research interests.

The concept of skyrmion comes from a model for baryons in nuclear physics [5] and has been regarded as a topological particle of great significance in condensed-matter physics as well. In AFM spinor BECs we can also predict the existence of the counterpart which corresponds to a metastable excitation, while in FM spinor condensate the phrase "coreless vortex" is adopted sometimes [6,7]. Bogoliubov–de Gennes equations are very useful to study the stability of such spin-textured states in cold-atom systems [8,9]. Thermal fluctuations, etc., can limit the skyrmion lifetime which is the key element to make sure we can observe, even manipulate skyrmions in BEC system. Previous experiments have already successfully created the skyrmion in both AFM (^{23}Na) [10,11] and FM (^{87}Rb) [12] condensates. The decay process into the ground state was also observed [11]. However, few discussions have been made on the exact temporal dynamics of skyrmions before reaching the thermal equilibrium. Here we focus on the pure spin-1 BEC system at zero temperature and study the time evolution behaviors starting from either AFM or FM states supporting the skyrmionic spin texture.

The paper is organized as follows. In Sec. II we introduce the concept of skyrmion (coreless vortex) in the spin-1 condensate for both AFM and FM cases, and in Sec. III we analytically discuss the possible decay of skyrmion (coreless vortex) originated from the breakdown of AFM (FM) phase in the dynamical process. Numerical simulations of the real-time evolution behaviors are made in Sec. IV to show the detailed decay phenomena. Three different initial configurations are considered, exhibiting different evolution patterns. Finally, in Sec. V we summarize our results and present corresponding discussions.

II. GROUND STATE AND SKYRMION

In the mean-field approximation, the energy functional for the spin-1 condensate without the trapping potential is commonly given by [2,3]

$$E[\Psi] = \frac{\hbar^2}{2m}\int (\nabla\Psi^\dagger)\cdot(\nabla\Psi) + \frac{1}{2}\int \rho^2[c_0 + c_2(\mathbf{S})^2], \tag{1}$$

where $c_0 = (a_0 + 2a_2)4\pi\hbar^2/m$ and $c_2 = (a_2 - a_0)4\pi\hbar^2/m$ characterize the interaction strengths, a_i $(i = 0,2)$ are the s-wave scattering length in the two-atom ith scattering channel, and m is the particle mass. The spin-1 condensate wave function can be decomposed as

$$\Psi(\rho,\theta,\boldsymbol{\eta}) = \sqrt{\rho}e^{i\theta}\boldsymbol{\eta}, \tag{2}$$

where ρ and θ are the total density and overall phase and $\mathbf{S} = \boldsymbol{\eta}^\dagger\mathbf{F}\boldsymbol{\eta}$ describes the spin vector with $\boldsymbol{\eta}$ the unit-modulus spinor field obeying $\boldsymbol{\eta}^\dagger\boldsymbol{\eta} = 1$. The 3×3 angular momentum operator for spin-1 condensate is represented by $\mathbf{F} = \{F_x, F_y, F_z\}$. It is a common practice to distinguish the two regimes of the ground state according to c_2 being repulsive or attractive. The former corresponds to the AFM case where the spin average becomes zero, $|\mathbf{S}| = 0$, to minimize the spin-dependent interaction energy, whereas the latter is the FM case and the spin average is maximized, $|\mathbf{S}| = 1$. With the aid of spin rotation operator $\mathcal{U}(\alpha,\beta,\gamma) = e^{-iF_z\alpha}e^{-iF_y\beta}e^{-iF_z\gamma}$, where α, β, and γ are the Euler angles, we may express the two fields as [2,3]

$$\boldsymbol{\eta}_1 = \mathcal{U}\begin{pmatrix}0\\1\\0\end{pmatrix} = \begin{pmatrix}-\frac{1}{\sqrt{2}}e^{-i\alpha}\sin\beta\\ \cos\beta\\ \frac{1}{\sqrt{2}}e^{i\alpha}\sin\beta\end{pmatrix},$$
$$\boldsymbol{\eta}_2 = \mathcal{U}\begin{pmatrix}1\\0\\0\end{pmatrix} = e^{-i\gamma}\begin{pmatrix}e^{-i\alpha}\cos^2\frac{\beta}{2}\\ \frac{1}{\sqrt{2}}\sin\beta\\ e^{i\alpha}\sin^2\frac{\beta}{2}\end{pmatrix}. \tag{3}$$

*hanjh@skku.edu

Throughout the paper we denote $\boldsymbol{\eta}_1$ and $\boldsymbol{\eta}_2$ for AFM and FM order parameter manifolds, respectively. The two angular variables α and β can be used to construct a unit vector $\mathbf{d} = (\sin\beta\cos\alpha, \sin\beta\sin\alpha, \cos\beta)$, which, in turn, can give rise to a topological spin texture of the skyrmion (coreless vortex), where the integer $Q = \int dxdy\, \mathbf{d}\cdot(\partial_x\mathbf{d}\times\partial_y\mathbf{d})/(4\pi)$ denotes the topological charge. Typically, skyrmions refer to a configuration where the Euler angle α corresponds to the azimuthal angle ϕ of the plane, and β is a function of radial distance r varying from 0 at the origin, to π at infinity or the boundary of the condensate. Skyrmions can be imprinted in spinor BECs by a spin rotation method. In a recent experiment [11], the skyrmion created in the AFM ^{23}Na condensate decays into the ground state over time, producing what appears to be a half-quantum vortex-antivortex pair [13] within the condensate in the intermediate phase. Motivated by the dichotomy of the (theoretically) expected topological stability of the skyrmion in the AFM BEC and its smooth decay found in the experiment, it is a timely exercise to carry out a more critical analysis of the skyrmion dynamics in the spin-1 condensate.

III. EQUATION OF MOTION ANALYSIS

Some "pathology" in the spin-1 AFM dynamics was in fact noted early on [14]. The kinetic energy obtained for the AFM wave function Ψ_1 reads

$$E_1 = \frac{\hbar^2}{2m}\int \rho[(\nabla\mathbf{d})^2+(\nabla\theta)^2]+(\nabla\sqrt{\rho})^2, \tag{4}$$

while the action part $S_1 = i\int\Psi_1^\dagger\partial_t\Psi_1$ becomes $S_1 = -\int\rho\partial_t\theta$. As it happens, there is no term in the action responsible for the dynamics of the $\mathbf{d}$ vector. By contrast, the FM spinor wave function $\Psi_2 = \sqrt{\rho}e^{i\theta}\boldsymbol{\eta}_2$ gives rise to $S_2 = -\int\rho\partial_t\theta + \int(\cos\beta-1)\partial_t\alpha$, where the second term, Berry phase action, is responsible for the spin dynamics of $\mathbf{d}$ governed by the Landau-Lifshitz equation of motion. The discrepancy is further illustrated by the examination of the overlap integral between adjacently located wave functions $\Psi(\mathbf{r})$ and $\Psi(\mathbf{r}-\delta\mathbf{r})$ for the two cases [15,16],

$$\begin{aligned}&\Psi_1^\dagger(\mathbf{r}-\delta\mathbf{r})\Psi_1(\mathbf{r}) \simeq \rho(\mathbf{r}),\\ &\Psi_2^\dagger(\mathbf{r}-\delta\mathbf{r})\Psi_2(\mathbf{r}) \simeq \rho(\mathbf{r})e^{i\cos\beta(\nabla\alpha\cdot\delta\mathbf{r})}.\end{aligned} \tag{5}$$

The overlap of the adjacent FM wave functions produces the Berry phase factor, which is absent for AFM wave-function overlap.

A way to cure the pathology of the $\mathbf{d}$-vector dynamics in the AFM manifold was suggested by the authors of Ref. [14], who considered small fluctuations away from the AFM manifold and obtained, by integrating out the fluctuations, an effective action for $\mathbf{d}$ that is quadratic in time $\sim(\partial\mathbf{d}/\partial t)^2$, rather than first-order, as expected in superfluid vortices [15,16] and magnetic skyrmions [17,18]. A similar idea was explored by Ruostekoski and Anglin, who numerically observed the spontaneous deformation of the monopole core into an extended defect called the Alice string, and attributed the phenomenon to the energetic balance of AFM and non-AFM components in the wave function [19].

Here we want to offer another perspective of this dynamical problem. When we define the spinor fields in Eq. (3), we rotated the two bases $(0,1,0)^T$ and $(1,0,0)^T$, but ignored the third one $(0,0,1)^T$. Euler rotation of this third basis yields

$$\boldsymbol{\eta}_3 = \mathcal{U}\begin{pmatrix}0\\0\\1\end{pmatrix} = e^{i\gamma}\begin{pmatrix}e^{-i\alpha}\sin^2\frac{\beta}{2}\\ -\frac{1}{\sqrt{2}}\sin\beta\\ e^{i\alpha}\cos^2\frac{\beta}{2}\end{pmatrix}, \tag{6}$$

which also corresponds to the FM manifold. Together the three fields $\boldsymbol{\eta}_j$ $(j=1,2,3)$ form a complete, orthogonal set obeying $\boldsymbol{\eta}_j^\dagger\boldsymbol{\eta}_k = \delta_{jk}$. An arbitrary spinor $\boldsymbol{\eta}$ must therefore be a linear combination of the three basis vectors. Now we consider the initial AFM or FM state and let it evolve for a small time step Δt to see the composition of the intermediate state, that is, $\Psi(\Delta t)-\Psi(0)\approx -i\Delta t H(0)\Psi(0)$, where $H = -\hbar^2\nabla^2/(2m) + c_0\Psi^\dagger\Psi + c_2(\Psi^\dagger\mathbf{F}\Psi)\cdot\mathbf{F}$.

First, for the AFM state we set $\Psi(0)=\boldsymbol{\eta}_1$, and the action of the Hamiltonian on it yields

$$H\boldsymbol{\eta}_1 = -\frac{\hbar^2}{2m}\nabla^2\boldsymbol{\eta}_1 + c_0\boldsymbol{\eta}_1 = u_j\boldsymbol{\eta}_j, \tag{7}$$

with

$$\begin{aligned}u_1 &= \frac{\hbar^2}{2m}[(\partial_i\beta)^2+(\partial_i\alpha)^2\sin^2\beta]+c_0,\\ u_2 &= -\frac{\hbar^2}{2m}(A_1+A_2+A_3-A_4)e^{i\gamma},\\ u_3 &= -\frac{\hbar^2}{2m}(-A_1+A_2+A_3+A_4)e^{-i\gamma},\end{aligned} \tag{8}$$

where we have defined $A_1 = (\partial_i\alpha)^2\sin\beta\cos\beta/\sqrt{2}$, $A_2 = i(\partial_i^2\alpha)\sin\beta/\sqrt{2}$, $A_3 = i\sqrt{2}(\partial_i\alpha)(\partial_i\beta)\cos\beta$, and $A_4 = \partial_i^2\beta/\sqrt{2}$. Note that the Einstein convention is used, and $i = x,y$ for two dimensions. In general, u_j $(j=1,2,3)$ are nonzero. As a result, the initial pure AFM state would evolve into the mixture containing the FM component. The disappearance of c_2 in u_j indicates that c_2 plays no role in the beginning of the evolution.

For the FM initial state, $\Psi(0)=\boldsymbol{\eta}_2$, we have

$$H\boldsymbol{\eta}_2 = -\frac{\hbar^2}{2m}\nabla^2\boldsymbol{\eta}_2 + c_0\boldsymbol{\eta}_2 + c_2\mathbf{d}\cdot\mathbf{F}\boldsymbol{\eta}_2 = v_j\boldsymbol{\eta}_j, \tag{9}$$

with

$$\begin{aligned}v_1 = -\frac{\hbar^2}{2m}\Big\{&\frac{1}{\sqrt{2}}[2(\partial_i\alpha)(\partial_i\gamma)+i\partial_i^2\gamma]\sin\beta\\ &-\frac{i}{\sqrt{2}}[2(\partial_i\beta)(\partial_i\gamma)+i\partial_i^2\beta]\\ &+\frac{1}{\sqrt{2}}(\partial_i\alpha)^2\sin\beta\cos\beta\Big\}e^{-i\gamma},\\ v_2 = -\frac{\hbar^2}{2m}&(-B_1-B_2+B_3-B_4-B_5-B_6)+c_0+c_2,\\ v_3 = -\frac{\hbar^2}{2m}&(-B_1+B_2+B_3+B_4-B_5+B_6)e^{-2i\gamma},\end{aligned} \tag{10}$$

where we have $B_1 = [(\partial_i\alpha)^2+(\partial_i\gamma)^2+i\partial_i^2\alpha]/2$, $B_2 = [2(\partial_i\alpha)(\partial_i\gamma)+i\partial_i^2\gamma](\cos\beta)/2$, $B_3 = i(\partial_i\beta)(\partial_i\alpha)\sin\beta$,

$B_4 = [(\partial_i\beta)^2 + i\partial_i^2\gamma + (\partial_i\gamma)^2]/2$, $B_5 = [2(\partial_i\alpha)(\partial_i\gamma) + i\partial_i^2\alpha](\cos\beta)/2$, and $B_6 = (\partial_i\alpha)^2(\cos^2\beta)/2$. Immediately, we can draw the conclusion that the initial pure FM state would also be mixed with AFM component during the time evolution. Additionally, positive (negative) c_2 may enhance (reduce) the effects of c_0, which will be further confirmed later.

The main lesson of the above short-time analysis is that we can readily deduce the source of AFM-FM mixing to be mainly the inhomogeneity in α and β, that is to say, the kinetic energy carried by the inhomogeneous initial condensate wave function. It is the spin texture in the initial configuration which drives the mixing. A textured localized object such as a skyrmion (coreless vortex) in a pure AFM (FM) condensate inevitably evolves into a mixed phase due to its intrinsic inhomogeneity.

IV. DESCRIPTION OF NUMERICS

Exact time evolution behavior can be obtained by numerically solving the full set of Gross-Pitaevskii (GP) equations in the presence of a trap,

$$i\frac{\partial}{\partial t}\Psi = \left(-\frac{\hbar^2\nabla^2}{2m} + V + c_0(\Psi^\dagger\Psi) + c_2(\Psi^\dagger\mathbf{F}\Psi)\cdot\mathbf{F}\right)\Psi, \tag{11}$$

where $V = m\omega^2\mathbf{r}^2/2$ ($\mathbf{r} = x\mathbf{e}_x + y\mathbf{e}_y$) is the two-dimensional harmonic trapping potential. To make all quantities dimensionless we set the energy, length, and time scales as $\hbar\omega$, $\sqrt{\hbar/m\omega}$, and $1/\omega$, respectively. As we are mainly interested in the skyrmion (coreless vortex) dynamics in the spin-1 condensate, initial states are chosen to be either $\Psi_{\rm AFM}(\mathbf{r},0) = \sqrt{\rho(\mathbf{r}-\boldsymbol{\xi}_\rho)}\boldsymbol{\eta}_1(\mathbf{r}-\boldsymbol{\xi}_{\rm s})$ or $\Psi_{\rm FM}(\mathbf{r},0) = \sqrt{\rho(\mathbf{r}-\boldsymbol{\xi}_\rho)}\boldsymbol{\eta}_2(\mathbf{r}-\boldsymbol{\xi}_{\rm s})$, which represent the skyrmion (coreless vortex) in a pure AFM (FM) state. For general consideration we introduce the displacement of the density peak from the trap center by $\boldsymbol{\xi}_\rho$, while $\boldsymbol{\xi}_{\rm s}$ is the displacement of skyrmionic spin texture. We assume both $\boldsymbol{\xi}_\rho$ and $\boldsymbol{\xi}_{\rm s}$ are small quantities (compared to the condensate size) in the x direction; that is, $\boldsymbol{\xi}_\rho = \xi_\rho\mathbf{e}_x$ and $\boldsymbol{\xi}_{\rm s} = \xi_{\rm s}\mathbf{e}_x$. The density distribution takes the Gaussian profile $\rho(\mathbf{r}-\boldsymbol{\xi}_\rho) = e^{-(\mathbf{r}-\boldsymbol{\xi}_\rho)^2}/\sqrt{2\pi}$, which is the single-particle ground state in the harmonic trapping potential. Our choice of the density profile is not the exact many-body ground (or metastable) state of the given Hamiltonian. For the sake of evolution, derivation from such an exact state is desired; therefore, we choose the current form for simplicity. For the AFM spinor fields we have

$$\boldsymbol{\eta}_1 = \begin{pmatrix} -\frac{1}{\sqrt{2}}e^{-i\phi(\mathbf{r}-\boldsymbol{\xi}_{\rm s})}\sin\beta(\mathbf{r}-\boldsymbol{\xi}_{\rm s}) \\ \cos\beta(\mathbf{r}-\boldsymbol{\xi}_{\rm s}) \\ \frac{1}{\sqrt{2}}e^{i\phi(\mathbf{r}-\boldsymbol{\xi}_{\rm s})}\sin\beta(\mathbf{r}-\boldsymbol{\xi}_{\rm s}) \end{pmatrix}, \tag{12}$$

where $\phi(\mathbf{r}-\boldsymbol{\xi}_{\rm s})$ is the azimuthal angle, and $\cos\beta(\mathbf{r}-\boldsymbol{\xi}_{\rm s}) = [(\mathbf{r}-\boldsymbol{\xi}_{\rm s})^2 - 1]/[(\mathbf{r}-\boldsymbol{\xi}_{\rm s})^2 + 1]$, $\sin\beta(\mathbf{r}-\boldsymbol{\xi}_{\rm s}) = 2|\mathbf{r}-\boldsymbol{\xi}_{\rm s}|/[(\mathbf{r}-\boldsymbol{\xi}_{\rm s})^2 + 1]$ is used. For the FM case, in view of the recent experiment [12], we may adopt

$$\boldsymbol{\eta}_2 = \begin{pmatrix} \cos^2\frac{\beta(\mathbf{r}-\boldsymbol{\xi}_{\rm s})}{2} \\ \frac{1}{\sqrt{2}}e^{i\phi(\mathbf{r}-\boldsymbol{\xi}_{\rm s})}\sin\beta(\mathbf{r}-\boldsymbol{\xi}_{\rm s}) \\ e^{2i\phi(\mathbf{r}-\boldsymbol{\xi}_{\rm s})}\sin^2\frac{\beta(\mathbf{r}-\boldsymbol{\xi}_{\rm s})}{2} \end{pmatrix}, \tag{13}$$

where $\beta(\mathbf{r}-\boldsymbol{\xi}_{\rm s}) = \pi(1 - e^{-|\mathbf{r}-\boldsymbol{\xi}_{\rm s}|})$ varies from 0 to π. Note that similar results are always obtained regardless of the choice of the exact radial dependence of β. We may define $\Psi = (\psi_{+1},\psi_0,\psi_{-1})^T$, where ψ_i ($i = +1,0,-1$) denote the wave functions in the corresponding hyperfine states. Initially, the winding numbers of ψ_{+1}, ψ_0, and ψ_{-1} for AFM and FM cases are $(-1,0,1)$ and $(0,1,2)$, respectively. In the following calculations, the real-time evolution method is used, and we set $c_0 = 50.0$. Considering the possible experimental setup, we discuss the following three kinds of situations with regard to different choices of ξ_ρ and $\xi_{\rm s}$.

A. $\xi_\rho = \xi_{\rm s} = 0$

In this case, both the density and the skyrmionic texture are centered, enabling the rotational symmetry to be preserved during the whole evolution process. As discussed in Sec. III, either a pure AFM or a pure FM initial state will evolve into a mixture of both components. Indeed, as shown in Fig. 1(a), nonzero $|\mathbf{S}(\mathbf{r},t)|$ ($t > 0$) indicates the appearance of the FM feature out of the AFM initial state, while in Fig. 1(b), the deviation of $|\mathbf{S}(\mathbf{r},t)|$ from 1 shows the loss of FM character although the initial state was fully FM.

Naturally it becomes problematic to give the precise meaning to the skyrmion now that the very manifold (either AFM or FM) on which it was defined gets disintegrated over time. It might be possible, through decomposition of the condensate wave function in the basis space spanned by $\boldsymbol{\eta}_j$ ($j = 1,2,3$) as introduced in the previous section, to deduce the $\mathbf{d}(\mathbf{r},t)$ vector and the skyrmion density $\mathbf{d}\cdot(\partial_x\mathbf{d}\times\partial_y\mathbf{d})/4\pi$ formally at any given time t for any wave function $\Psi(\mathbf{r},t)$. This is a subtle and important issue which we will treat in a later publication. In the mixed AFM and FM state, the winding numbers of ψ_i ($i = +1,0,-1$) are still preserved during the evolution, and the vortex (antivortex) cores always coincide with each other. Since some skyrmionic features continue to be maintained over time, we may name this structure in the mixed state a "pseudoskyrmion" for the convenience of description.

B. $\xi_\rho = 0$ and $\xi_{\rm s} > 0$

In the previous section the initial skyrmionic configuration obeyed the rotational symmetry. The subsequent disintegration of the AFM or FM component was largely due to the inherent dynamics of the condensate, unrelated to effects arising from

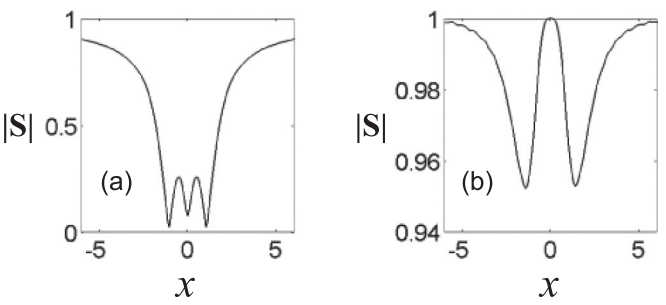

FIG. 1. Radial dependence of $|\mathbf{S}(x,y=0,t)|$ for the initial skyrmionic configuration defined on (a) AFM and (b) FM manifolds taken at time $t = 2.0$ with $c_2 = 0.0$. Other values of c_2 from -20 to 20 were tried, supporting similar results.

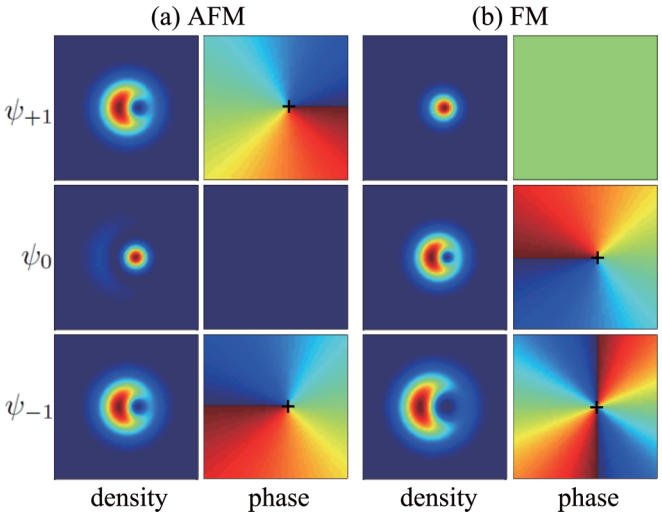

FIG. 2. (Color online) Initial density and phase profiles for a displaced skyrmion within the AFM manifold (a) and those of a displaced coreless vortex within the FM manifold (b). The top, middle, and bottom rows correspond to ψ_{+1}, ψ_0, and ψ_{-1}, respectively. Initial displacements are both at $\xi_s = 0.5$. The plus signs (+) mark the positions of vortex (antivortex) cores.

the trap potential. Now we consider the case when the skyrmion (coreless vortex) is initially displaced from the trap center. In the spin rotation method as adopted in Ref. [11], by tuning the position of the zero-field center of the three-dimensional quadrupole magnetic field, we may manipulate the position of the skyrmion (coreless vortex). Therefore, our setup is experimentally feasible. As a comparison, for a single-component condensate it is well known that a displaced vortex would precess around the trap core driven by a radial buoyant force and a gyroscopic Magnus force together [20].

For our spin-1 AFM initial state as shown in Fig. 2(a), the antivortex of ψ_{+1} and vortex of ψ_{-1} are located at the same position $\boldsymbol{\xi}_s$. However, they feel the opposite forces, and move in opposite directions, as shown in Figs. 3(a)–3(f). Note that similar behavior in the displaced AFM monopole dynamics of spin-1 condensate was discussed in Ref. [21]. The splitting of the vortex and the antivortex cores implies that a description of the condensate wave function based purely on AFM manifold is no longer tenable. To quantify the breakdown of the AFM phase, we define

$$f_{\mathrm{AFM}}(t) = \frac{\int dxdy\, ||\psi_{+1}(\mathbf{r},t)|^2 - |\psi_{-1}(\mathbf{r},t)|^2|}{\int dxdy\, ||\psi_{+1}(\mathbf{r},t)|^2 + |\psi_{-1}(\mathbf{r},t)|^2|} \qquad (14)$$

as a measure of the loss of the AFM component. Pure AFM condensate would obey $|\psi_{+1}(\mathbf{r},t)|^2 - |\psi_{-1}(\mathbf{r},t)|^2| = 0$. In Fig. 3(g) the obvious trend of increase of $f_{\mathrm{AFM}}(t)$ from zero confirms our picture that vortex-antivortex core separation implies the loss of AFM condensate. As $t \to 0$, the effects of c_2 caused by its value and sign are reduced, as clear from the figure, confirming the analysis in Sec. III.

The simulation results suggest another way for the initial skyrmion structure to disintegrate. The inherent dynamics of the vortex in the superfluid follows that of electrons in quantized magnetic field [15,16]. The trapping potential provides the confining force, the analog of electric field, for

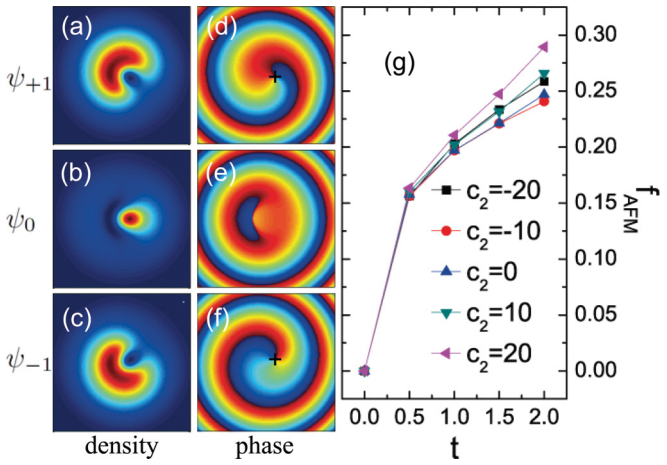

FIG. 3. (Color online) Real-time evolution starting from a displaced skyrmion within the AFM initial manifold as shown in Fig. 2(a) for $c_2 = 0.0$. (a)–(c) Snapshots of densities of ψ_{+1}, ψ_0, and ψ_{-1}, respectively, at $t = 2.0$; (d)–(f) are the corresponding phases. The plus signs (+) mark the positions of vortex (antivortex) cores. (g) Time dependence of $f_{\mathrm{AFM}}(t)$ for different values of c_2.

the vortex so that the drift motion orthogonal to the confining force occurs. The charge of the vortex is opposite to that of the antivortex, so the drifts occur in opposite directions. Unless there exists an enormous force binding the vortex and the antivortex cores together, the drift mechanism will inevitably separate them in opposite directions and results in disintegration of the skyrmion.

As for the FM initial state in Eq. (13), both vortices in ψ_0 and ψ_{-1} have the same sign of the vorticity as seen from Fig. 2(b). Therefore, their cores move in the same direction when initially displaced from the trap center, as shown in Figs. 4(a)–4(f). During the evolution we observe that the $l = 2$ vortex in ψ_{-1} is unstable and decays into two $l = 1$ vortices, as shown in Figs. 4(c) and 4(f) [8,9]. To characterize the decay

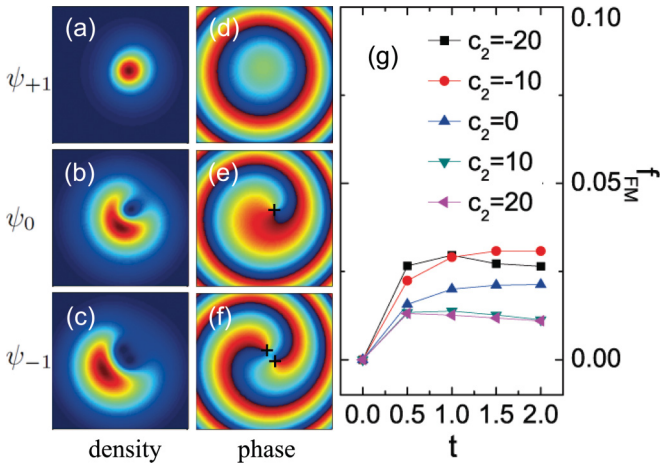

FIG. 4. (Color online) Real-time evolution starting from a displaced coreless vortex within the FM initial manifold as shown in Fig. 2(b) for $c_2 = 0.0$. (a)–(c) Snapshots of densities of ψ_{+1}, ψ_0, ψ_{-1}, respectively, at $t = 2.0$; (d)–(f) are the corresponding phases. The plus signs (+) mark the positions of vortex cores. (g) Time dependence of $f_{\mathrm{FM}}(t)$ for different values of c_2.

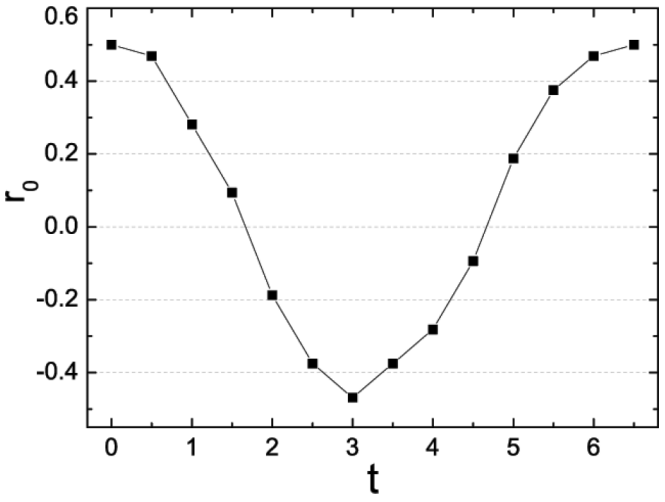

FIG. 5. Time dependence of the pseudoskyrmion displacement from the trap center for both AFM and FM initial states. The difference between the two is too small to distinguish here. Initial displacements are $\xi_\rho = \xi_s = 0.5$, and $c_2 = 0.0$. Other values of c_2 from -20 to 20 lead to similar quasiperiodic behaviors.

of the FM feature we define [22]

$$f_{\rm FM}(t) = \frac{\int dxdy(|\psi_{+1}(\mathbf{r},t)| + |\psi_{-1}(\mathbf{r},t)| - \sqrt{\rho})^2}{\int dxdy(|\psi_{+1}(\mathbf{r},t)| + |\psi_{-1}(\mathbf{r},t)| + \sqrt{\rho})^2}. \quad (15)$$

The definition is motivated by the observation that, in perfect FM state, $|\psi_{+1}(\mathbf{r},t)| + |\psi_{-1}(\mathbf{r},t)| = \sqrt{\rho}$ is guaranteed. From Fig. 4(g) we can observe the obvious trend of increase of $f_{\rm FM}(t)$ from zero. Another conclusion from the figure is that the positive c_2 may enhance the stiffness of the initial FM manifold, while the negative c_2, on the contrary, would favor faster speed of the disintegration from the FM state.

C. $\xi_\rho = \xi_s > 0$

Now we consider the case when the center of the density is displaced together with that of the skyrmionic texture. This situation is also realizable in experiments. First, we create a skyrmion (coreless vortex) centered in the harmonic trap following the standard procedure. After that we suddenly shift the trapping potential; therefore, both the density and the skyrmion (coreless vortex) core would be displaced with respect to the new trap center. During the time evolution the whole condensate moves like a pendulum about the trap center, accompanied by the disintegration of initial AFM or FM states. Contrary to the splitting of vortex-antivortex pair or the breakdown of $l = 2$ vortex seen in the previous section, now the pseudoskyrmion structure is always protected throughout the evolution for both two initial configurations. We show in Fig. 5 the time dependence of the displacement of the pseudoskyrmion from the trap center, where the periodic behavior with only one period of oscillation is presented. We may approximately describe the periodic motion of the pseudoskyrmion as the semiclassical Newtonian equation of motion [14]. We conclude that here the dynamics of the density ρ dominates over that of the spin texture and effectively acts as a binding force tying the vortex and antivortex cores together. Due to the nonlinear interactions, deviation from the perfect periodicity is observed.

V. SUMMARY AND DISCUSSION

Motivated by the recent experiment of skyrmion creation and its evolution in the AFM spin-1 condensate of ^{23}Na [11], we have carried out a detailed study of the skyrmion (coreless vortex) dynamics based on the GP equation analysis. Contrary to the standard notion of a skyrmion as a metastable topological object in, for example, a nonlinear σ model [23], it is *inherently unstable in the BEC condensate* due to the *dynamical mixing* of the AFM and FM components during the time evolution. The instability has a different character from that expected in thermal or quantum tunneling of the topological object out of the metastable minimum ("fate of the false vacuum") [24]. Interaction effects are also examined during the early stage of time evolution, exhibiting the explicit role of c_2 in the FM case and the independence of c_2 in the AFM counterpart.

Numerically, three feasible initial configurations have been investigated for their dynamical evolution behaviors. (i) For the skyrmion (coreless vortex) initially prepared in a pure AFM (FM) manifold and located at the trap center, the mixing with the FM (AFM) component is observed. The rotational symmetric structure is preserved over time. (ii) When we shift the skyrmion while keeping the density peaked at the center, splitting of the vortex and antivortex centers is observed for AFM initial state. Note that the AFM manifold breaks down at $t > 0$. For the FM initial coreless vortex state, the $l = 2$ vortex breaks up into two $l = 1$ vortices, while rotating around the trap center in the same direction. This also contributes to the breakdown of the FM manifold. (iii) If both the density peak and the skyrmion (coreless vortex) are displaced by the same amount, the whole condensate including the pseudoskyrmion oscillates through the trap center in analogy to the pendulum motion. The dynamics is governed by that of the density oscillation as a whole, not by those of individual vortices.

Given that our results rely on the energy-conserving simulation, they could not be applied directly to explain the transition into the ground state in Ref. [11]. However, before the system reaches its thermal equilibrium, short-time behaviors as discussed in our paper may be observable in experiments.

ACKNOWLEDGMENTS

H.J.H. is supported by NRF Grants No. 2010-0008529 and No. 2011-0015631. We acknowledge useful communication with Y. Shin on the skyrmion decay and his experimental input.

[1] D. M. Stamper-Kurn, M. R. Andrews, A. P. Chikkatur, S. Inouye, H.-J. Miesner, J. Stenger, and W. Ketterle, Phys. Rev. Lett. **80**, 2027 (1998).

[2] T.-L. Ho, Phys. Rev. Lett. **81**, 742 (1998).

[3] T. Ohmi and K. Machida, J. Phys. Soc. Jpn. **67**, 1822 (1998).

[4] M.-S. Chang, Q. Qin, W. Zhang, L. You, and M. S. Chapman, Nat. Phys. **1**, 111 (2005).
[5] T. H. R. Skyrme, Proc. R. Soc. London, Ser. A **260**, 127 (1961); Nucl. Phys. **31**, 556 (1962).
[6] U. A. Khawaja and H. T. C. Stoof, Nature (London) **411**, 918 (2001); Phys. Rev. A **64**, 043612 (2001); H. Zhai, W. Q. Chen, Z. Xu, and L. Chang, *ibid.* **68**, 043602 (2003).
[7] J. Choi, W. J. Kwon, M. Lee, H. Jeong, K. An, and Y. Shin, New J. Phys. **14**, 053013 (2012).
[8] V. Pietilä, M. Möttönen, and S. M. M. Virtanen, Phys. Rev. A **76**, 023610 (2007).
[9] M. Takahashi, V. Pietilä, M. Möttönen, T. Mizushima, and K. Machida, Phys. Rev. A **79**, 023618 (2009).
[10] A. E. Leanhardt, Y. Shin, D. Kielpinski, D. E. Pritchard, and W. Ketterle, Phys. Rev. Lett. **90**, 140403 (2003).
[11] J. Y. Choi, W. J. Kwon, and Y. I. Shin, Phys. Rev. Lett. **108**, 035301 (2012).
[12] L. S. Leslie, A. Hansen, K. C. Wright, B. M. Deutsch, and N. P. Bigelow, Phys. Rev. Lett. **103**, 250401 (2009).
[13] J. Lovegrove, M. O. Borgh, and J. Ruostekoski, Phys. Rev. A **86**, 013613 (2012).
[14] H. T. C. Stoof, E. Vliegen, and U. Al Khawaja, Phys. Rev. Lett. **87**, 120407 (2001).
[15] F. D. M. Haldane and Y.-S. Wu, Phys. Rev. Lett. **55**, 2887 (1985).
[16] Q. Niu, P. Ao, and D. J. Thouless, Phys. Rev. Lett. **72**, 1706 (1994).
[17] M. Stone, Phys. Rev. B **53**, 16573 (1996).
[18] J. Zang, M. Mostovoy, J. H. Han, and N. Nagaosa, Phys. Rev. Lett. **107**, 136804 (2011).
[19] J. Ruostekoski and J. R. Anglin, Phys. Rev. Lett. **91**, 190402 (2003).
[20] D. V. Freilich, D. M. Bianchi, A. M. Kaufman, T. K. Langin, and D. S. Hall, Science **329**, 1182 (2010).
[21] J.-P. Martikainen, A. Collin, and K.-A. Suominen, Phys. Rev. Lett. **88**, 090404 (2002).
[22] The choice of $f_{\mathrm{AFM}}(t)$ and $f_{\mathrm{FM}}(t)$ is not unique. Other definitions measuring AFM or FM fractions can be given, presumably with similar results. The arbitrariness is obviously related to the lack of well-defined procedure to extract AFM and FM components out of the spin-1 spinor wave function.
[23] R. Rajaraman, *Solitons and Instasntons* (North-Holland, Amsterdam, 1987), Chap. 3.
[24] S. Coleman, *Aspects of Symmetry* (Cambridge University Press, Cambridge, 1988), Chap. 7.